ISSN: 0067-2904

Role of the Center of Mass Correction in Magnetic Form Factors for ^{19}O and ^{21}Na Exotic Nuclei with Different Interactions

M. H. Hawi[1]*, Z. A. Dakhil[1] and B. S. Hameed[2]
[1]*Department of Physics, College of Science, University of Baghdad, Baghdad, Iraq*
[2]*Department of Physics, College of Science for Women, University of Baghdad, Baghdad, Iraq*

Received: 7/8/2022 Accepted: 27/3/2023 Published: 30/3/2024

Abstract

The transverse magnetic electron scattering form factors of ^{19}O and ^{21}Na exotic nuclei were studied in the plane wave Born approximation (PWBA). The shell model calculations with three *sd*-shell interactions, USDA, USDB, and Wildenthal, were carried out for the ground and low-lying excited states. The exact center of mass correction in the Born approximation picture through the translation-invariant shell model (TISM) was included to modify the transverse form factors. The measured magnetic dipole moments were well reproduced with the core polarization (CP) effect introduced through the effective g-factors. The occupancies percentage with respect to the valence nucleons was also calculated.

Keywords: Shell model, Exotic nuclei, Electro-magnetic transition, Magnetic dipole moment.

دور تصحيح مركز الكتلة في عوامل التشكل المغناطيسية للنوى الغريبة ^{19}O و ^{21}Na بإستخدام تفاعلات مختلفة

مرتضى هادي حاوي[1]*، زاهدة أحمد دخيل[1] و بان صباح حميد[2]
[1]قسم الفيزياء، كلية العلوم، جامعة بغداد، بغداد، العراق
[2]قسم الفيزياء، كلية العلوم للبنات، جامعة بغداد، بغداد، العراق

الخلاصة

تمت دراسة عوامل تشكل الإستطارة الإلكترونية المستعرضة للنوى الغريبة ^{19}O و ^{21}Na وفق تقريب بورن للموجة المستوية. إنجزت حسابات أنموذج القشرة بإستخدام تفاعلات القشرة *sd*–shell الثلاث USDA ,USDBو Wildenthal للحالات الأرضية و المتهيجة المنخفضة . أدخل تصحيح مركز الكتلة المضبوط وفق تقريب بورن من خلال أنموذج الأغلفة غير المعتمد على حركة مركز الكتلة لتعديل عوامل التشكل المستعرضة. تم تفسير العزوم ثنائية القطب المغناطيسية المقاسة بشكل جيد بإدخال تأثير استقطاب القلب من خلال عوامل– g الفعالة. تم أيضا حساب النسبة المئوية لأعداد الإشغال نسبة إلى نويات التكافؤ.

*Email: phymurteza@gmail.com;

1. Introduction

Electron-nucleus scatterings are the main probes to gain very good information about the nuclear structure of stable and unstable nuclei. The key benefits of using electrons as probes are attributed to the electromagnetic interaction properties, which are accurately represented by quantum electrodynamics–QED [1]. Elastic magnetic electron scattering is widely used to study the valence structure of the nuclei near the stability line [2].

The magnetic moment is very sensitive to the single-particle orbits occupied by the unpaired nucleons. Consequently, this quantity may also give the means to distinguish between spherical and deformed states [3,4]. The investigation of the properties of exotic nuclei becomes one of the most important goals in nuclear physics [5].

The latest developments in radioactive beams have opened up many new avenues in the physics of exotic nuclei. Simultaneously, it becomes increasingly important to establish theoretical models that can aid in data interpretation [6]. The study of exotic nuclei is at the forefront of research in nuclear physics because it cannot only discover new nuclear properties and thereby enrich our knowledge of atomic nuclei but also allows the understanding of the nucleosynthesis origin of chemical elements [7]. Jakubassa-Amundsen [8] calculated differential cross-sections and polarization correlations for the scattering of relativistic spin-polarized leptons from the unpolarized ground state of sodium (Na) nuclei within the distorted-wave Born approximation (DWBA). Various nuclear ground state charge distributions were probed. Besides, potential scattering, electric C2, and magnetic M1 and M3 transitions were taken into account. Sarriguren et al. [9,10] determined the form factors of the elastic magnetic electron scattering from odd-A nuclei in plane-wave Born approximation using a Skyrme HF+BCS method. The calculations have been carried out on several stable nuclei. Their results for deformed formalism improved the agreement with the experiment in deformed nuclei. Hudan et al. [11] presented the above-barrier fusion cross sections for an isotopic chain of oxygen isotopes with A = 16-19 incident on a ^{12}C target. Experimental data have been compared with both static and dynamic microscopic calculations. Their results suggest for neutron-rich nuclei existing time-dependent Hartree-Fock calculations underpredict the role of dynamics at near-barrier energies.

In the present work, three *sd*-shell interactions; USDA, USDB, and Wildenthal were used to calculate the magnetic transitions matrix elements and dipole moments of the ground and excited states of ^{19}O and ^{21}Na exotic nuclei.

Wildenthal Interaction USD Hamiltonian [12] has provided realistic *sd*-shell wave functions for use in models of nuclear structures, nuclear spectroscopy, and nuclear astrophysics. Also, Brown and Wildenthal [13] formulated the USD interaction for the *sd*-shell composed of three orbits: $1d_{5/2}$, $2s_{1/2}$, $1d_{3/2}$. Two interactions; universal *sd*-hell interaction A (USDA) and universal *sd*-shell interaction B (USDB), have been acquired by Brown and Richter [14]. For USDA 30 linear combinations of one- and two-body matrix elements were varied, while the remaining 36 linear combinations were fixed at a renormalized G-matrix value. For USDB, 56 linear combinations were varied with 10 fixed at values of G-matrix. They have utilized three *sd*-shell Hamiltonians (USD, USDA, and USDB) to study observables including M1, E2 moments, and transitions matrix elements, Gamow Teller (GT) β-decay matrix elements, and spectroscopic factors between ground states [15].

The present work aims to investigate the role of the center of mass correction on the transverse electron scattering form factors of ^{19}O and ^{21}Na exotic nuclei. The calculations of

this correction were based on the Translation Invariant Shell Model (TISM). The exact center-of-mass correction of Mihaila-Heisenberg [16] was adopted to generate the transverse form factors. The center of mass correction that was used in other previous works was also taken into account for comparison. The core polarization (CP) effects are included through the effective g-factors to reproduce the observable values of magnetic moments. The sensitivity of the transverse magnetic form factors and magnetic moments of the ground and low-lying states of ^{19}O and ^{21}Na were re-examined to the three *sd*-shell interactions; USDA, USDB, and Wildenthal (W).

2. Theoretical Formalism

The transverse form factor of multipolarity J as a function of momentum transfer in spin-isospin spaces can be expressed as [17]:

$$\left|F_J^{\eta}(q)\right|^2 = \frac{4\pi}{Z^2(2J_i+1)}\left|\sum_{T=0,1}(-1)^{T_f-T_{z_f}}\begin{pmatrix} T_f & T & T_i \\ -T_{zf} & M_T & T_{zi}\end{pmatrix}\left\langle J_f T_f \left\| \hat{T}_J^{\eta}(q) \right\| J_i T_i \right\rangle\right|^2 \times\left|F_{c.m}(q)\right|^2 \times\left|F_{f.s}(q)\right|^2 \quad (1)$$

The notation η represents the transverse (T) electric El or magnetic M. J_i and J_f are the total angular momentum of the initial and final states, respectively. $\hat{T}^{\eta}_J(q)$ is the electron scattering multipole operator, and $\langle\|\quad\|\rangle$ is the reduced matrix elements in both spin and isospin spaces.

The bracket $\begin{pmatrix}\cdot & \cdot & \cdot \\ \cdot & \cdot & \cdot\end{pmatrix}$ denotes the 3-*j* symbols. Since $T_{z_f} = T_{z_i}$ for electron scattering, then $M_T = 0$. Since the Hamiltonian in the shell model is, in general, not translation invariant [18], the center-of-mass correction is given by [19]: $F_{c.m.} = e^{\frac{q^2b^2}{4A}}$, Where b is the oscillator length parameter, and $\boldsymbol{A}$ is the nuclear mass number. The free nucleon correction due to the finite size of the nucleon takes the form [20]: $F_{f.s.}(q) = \left[1 + \left(\frac{q}{4.33}\ fm^{-1}\right)^2\right]^{-2}$.

The reduced matrix elements of the magnetic operator T^m_{JT} between the final and initial many nucleon states of the system including the configuration mixing can be written as the product sum of the one-body density matrix (OBDM)elements times the single-nucleon matrix elements [21]:

$$\left\langle J_f\ T_f \left\| \hat{T}^m_{J,T}(q) \right\| J_i\ T_i \right\rangle = \sum_{a,b} OBDM\left(J, J_f, J_i, a, b, t_z\right)\left\langle a \left\| \hat{T}^m_{J,t_z}(q) \right\| b \right\rangle \quad (2)$$

The sum extends over all pairs of single-nucleon states (*a*,*b*). The OBDM (ΔT) is defined in the second quantization notation as [22]:

$$OBDM\ (J,\ a,b,\ f,i,\Delta T) = \frac{\left\langle f \left\| \left[a^+_{(a)} \otimes \tilde{a}_{(b)}\right]^{(J,\Delta T)} \right\| i \right\rangle}{\sqrt{(2J+1)\ (2T+1)}} \quad (3)$$

The operators $\boldsymbol{a}^+$ and $\tilde{\boldsymbol{a}}$ are the creation and annihilation operators of a neutron or proton (according to the value of t_z) in the single states $\boldsymbol{a}$ and $\boldsymbol{b}$, respectively.

The average occupation numbers in each sub-shell j are given by [23]:

$$occ\#(j,t_z)=\sum_{a,b} OBDM\left(a,b,t_z,J=0\right)\sqrt{\frac{2j+1}{2J_i+1}} \tag{4}$$

The reduced single-nucleon matrix element of the magnetic operator T^m_{JT} is given by [24]:

$$\left\langle a \left\| \hat{T}^m_{J,t_z} \right\| b \right\rangle = i\mu_N \left[g_l(t_z)\, O^m_J(a,b) + g_S(t_z)\, S^m_J(a,b) \right] \tag{5}$$

Where: $\mu_N = \frac{e\hbar}{2m_p c} = 0.1051\ e.fm$ is the nuclear magneton, with the proton mass m_p. $g_l(t_z)$ and $g_s(t_z)$ are the orbital and spin-free nucleon g-factors, respectively. g_ℓ (1/2) = 1, g_s (1/2) = 5.585 for proton, and g_ℓ (-1/2) = 0, g_s (-1/2) = -3.826 for neutron. Also:

$$O^m_J(a,b) = P_J(m,l_a,l_b)\, C_J(j_a,j_b)\, A_J(j_a,j_b)$$
$$\times\sqrt{J(J+1)}\,\frac{q}{2J+1}\left\langle n_a l_a \left| \frac{1}{r}\, j_J(qr) \right| n_b l_b \right\rangle$$
$$S^m_J(a,b) = \frac{1}{2}\,[J(J+1)]^{-1/2}\, C_J(j_a,j_b)\, P_J(m,l_a,l_b)$$
$$\times\left\{ B(j_a,j_b)\,[\left\langle n_a l_a \left| j_J(qr)\, d/dr \right| n_b l_b \right\rangle + \left\langle n_b l_b \left| j_J(qr)\, d/dr \right| n_a l_a \right\rangle] \right.$$
$$\left. +\,[B(j_a,j_b) - J(J+1)]\left\langle n_a l_a \left| \frac{1}{r}\, j_J(qr) \right| n_b l_b \right\rangle \right\} \tag{6}$$

The coefficients C_J, P_J, and A_J are given by:

$$C_J(j_a,j_b) = (-1)^{j_a+\frac{1}{2}} \left[\frac{(2j_a+1)(2J+1)(2j_b+1)}{4\pi} \right]^{\frac{1}{2}} \begin{pmatrix} j_a & J & j_b \\ \frac{1}{2} & 0 & \frac{1}{2} \end{pmatrix} \tag{7}$$

$$P_J(m,l_a,l_b) = \frac{1}{2}\left[1 + (-1)^{l_a+l_b+J+1} \right] \tag{8}$$

$$B(a,b) = 2 + D(j_a,l_a) + D(j_b,l_b) \tag{9}$$

With, $D(j,l) = j\,(j+1) - l(l+1) - 3/4$

The magnetic dipole moment μ of a state of total angular momentum J is given by [21,24]:

$$\mu = \sqrt{\frac{4\pi}{3}} \begin{pmatrix} J_i & 1 & J_i \\ -J_i & 0 & J_i \end{pmatrix} \left\langle J_i \left\| \sum_{k=1}^{n} \hat{O}_k(m1) \right\| J_i \right\rangle \tag{10}$$

$$\left\langle J_i \left\| \sum_{k=1}^{n} \hat{O}_k(m1) \right\| J_i \right\rangle = \sum_{a,b,T} (-1)^{T_i - T_z} \begin{pmatrix} T_i & T & T_i \\ -T_z & 0 & T_z \end{pmatrix} OBDM(a,b,J=1,T) \left\langle a \left\| \hat{O}_T(m1) \right\| b \right\rangle \tag{11}$$

2.1. The Exact Center of Mass Correction in Translation Invariant Shell Model (TISM)

The Translation Invariant Shell Model (TISM) provides a proper description of the electron scattering process, the wave function factorizes into the center of mass wave function being a Gaussian and an intrinsic wave function of relative coordinates. This allows calculating the form factor in the form [16]:

$$F(q) = e^{(-1/4)b^2 q^2/A}\, F_{\text{int}}(q) \tag{12}$$

The calculation usually gives the form factor of one-body density labeled *F(q)*, whereas the experiment requires the form factors with respect to the center of mass, labeled F_{int} *(q)*. The form factor at momentum transfer q in Born approximation is given by [16,19]:

$$F_{\text{int}}(\vec{q}) = \left\langle \phi_\circ \left| \sum_k f_k(q^2)\, e^{i\vec{q}.\vec{r}_k'} \right| \phi_\circ \right\rangle \tag{13}$$

Where: $\boldsymbol{\phi}_\circ$ is the translation-invariant ground state, $\vec{r}_k'$ is the distance from the center of mass to the $\boldsymbol{k^{th}}$ "point" nucleon, $(\vec{r}_k' = \vec{r}_k - \vec{R}_{c.m})$, $\boldsymbol{k}$ *= 1, 2,...A-1,* and $f_k(q^2)$ is the nucleon form factor which takes into account the finite size of the nucleon $\boldsymbol{k}$. For an approximate model wave function $\Phi_\circ^M$, the decomposition can be obtained [26]:

$$\Phi_\circ^M(\vec{r}_1, \vec{r}_2, ..., \vec{r}_A) = e^{i\vec{P}.\vec{R}_{c.m}}\, \phi_\circ^M(\vec{r}_1', \vec{r}_2', ..., \vec{r}_{A-1}') \tag{14}$$

Which is almost correct to the extent that the motion of the intrinsic coordinates and the center of mass is not correlated. Then only the following factorization is possible [16]:

$$F(q) = F_{c.m.}(q)\, F_{int}(q) \tag{15}$$

Assuming that the TISM can provide a good description of the internal structure of the nucleus ($\Phi_\circ = \Phi_\circ^M$) with that approximation, Eq. (15) is valid with [27,28]:

$$F_{\text{int}}(\vec{q}) = \left\langle \Phi_\circ^M \left| \sum_k f_k(q^2)\, e^{i\vec{q}.(\vec{r}_k' - R_{c.m})} \right| \Phi_\circ^M \right\rangle \tag{16}$$

$$\text{And} \quad F_{c.m.}(\vec{q}) = \left\langle \Phi_\circ^M \left| e^{i\vec{q}.\vec{R}_{c.m.}} \right| \Phi_\circ^M \right\rangle \tag{17}$$

The form factor given in Eq. (16) can be calculated by carrying out an expansion in terms of many-body operators [26]:

$$F_{\text{int}}(\vec{q}) = \sum_k f_k(q^2) \left\langle e^{i\vec{q}.\vec{r}_k\,(A-1)/A} \prod_{m\neq k} e^{-i\vec{q}.\vec{r}_m/A} \right\rangle \tag{18}$$

Each exponential in Eq. (18) can be expressed in terms of the one-body operator which can be defined by [16]:

$$f(\vec{q}.\vec{r}_m) = e^{i\vec{q}\,.\,\vec{r}_m} - 1 \tag{19}$$

With this, Eq. (18) can be written as:

$$F_{\text{int}}(\vec{q}) = \sum_k f_k(q^2) \left\langle e^{i\vec{q}.\vec{r}_k\,(A-1)/A} \prod_{m\neq k} [\,1 + f^*(\vec{q}.\vec{r}_m/A)\,] \right\rangle \tag{20}$$

The many-body expansion for the form factor F_{int} takes the following form:

$$\begin{aligned} F_{\text{int}}(\vec{q}) = & \sum_k f_k(q^2) \left\langle e^{i\vec{q}.\vec{r}_k\,(A-1)/A} \right\rangle \\ & + \sum_k f_k(q^2) \sum_{m\neq k} \left\langle e^{i\vec{q}.\vec{r}_k\,(A-1)/A}\; f^*(\vec{q}.\vec{r}_m/A) \right\rangle \\ & + \tfrac{1}{2} \sum_k f_k(q^2) \sum_{m,n\neq k} \left\langle e^{i\vec{q}.\vec{r}_k\,(A-1)/A}\; f^*(\vec{q}.\vec{r}_m/A) \right\rangle \times f^*(\vec{q}.\vec{r}_n/A) + ... \end{aligned} \tag{21}$$

With the exact value of the center of mass correction introduced in TISM, the form factor given in Eq. (1) becomes:

$$\left|F_J^m(q)\right|^2 = \frac{4\pi}{Z^2(2J_i+1)}\left|\sum_{T=0,1}(-1)^{T_f-T_{fz}}\begin{pmatrix} T_f & T & T_i \\ -T_{zf} & M_T & T_{zi}\end{pmatrix}\left\langle J_f T_f \left\|\left\| \hat{T}_L^m(q) \right\|\right\| J_i T_i\right\rangle\right|^2$$
$$\times\left|F_{\text{int}}(q)\right|^2 \times \left|F_{f.s}(q)\right|^2 \quad (22)$$

In the present work, $F_{int}(q)$ was calculated from Eq. (21) and can be computed completely up to the third order in many-body expansion. More details were performed by Mihaila and Heisenberg [16]. The present calculations were carried out by use of the OXBASH shell model code [29].

3. Results and Discussion

The present study includes reexamining the center of mass correction (cm corr.) for the transverse form factors. The many-body expansion of Mihaila and Heisenberg [16] for the center of mass correction was applied to the case of Harmonic Oscillator (HO). The shell model calculations with *sd*-model space, and different interactions were performed for the ground and excited states of ^{19}O and ^{21}Na exotic nuclei. According to the multi-nucleon shell model with mixed configuration, the ^{19}O and ^{21}Na isotopes are considered the core of ^{16}O plus three and five residual nucleons divided over $1d_{5/2}$, $2s_{1/2}$, and $1d_{3/2}$, respectively. Three *sd*-shell interactions, USDA, USDB, and Wildenthal, were used to calculate the magnetic transitions matrix elements and dipole moments for the nuclei under consideration. The core-polarization effects were included through the effective g-factors. The magnetic dipole moments for the ground and excited states of ^{19}O and ^{21}Na exotic nuclei are listed in Table 1. The typical values of Richter et al. [15] were adopted with $g_l^p = 1.15$. $g_l^n = -0.15$. $g_s^{\frac{p}{n}} = 0.85$ g-free.

The occupation numbers of the valence nucleons were also determined. The single-particle wave functions of HO potential with the size parameter *b* were used. The size parameter *b* for exotic nuclei was obtained from the global formula for the HO length [22]: $b = \sqrt{\frac{\hbar}{M_p\,\omega}}$; $\hbar\omega = 45\,A^{-1/3} - 25\,A^{-2/3}$, where M_p is the proton mass.

3.1 ^{19}O nucleus ($J^\pi T = 5/2^+3/2$, $\tau_{1/2} = 27$ s)

The ground state of the ^{19}O (neutron-rich) nucleus can be considered as a core of ^{16}O with three additional neutrons distributed over $1d_{5/2}$, $2s_{1/2}$, and $1d_{3/2}$ orbits. The ground state of ^{19}O has the configurations of $(1s)^4$, $(1p_{3/2})^8$, $(1p_{1/2})^4$ inert core, with USDA interaction [15], as shown in Figure (1). This state is specified by $J^\pi T = 5/2^+3/2$ with a half-life of $\tau_{½} = 27$ s [30]. No experimental data are available for neutron-rich nuclei. The elastic transverse form factors with the $b_{rms} = 1.833$ fm were calculated for USDA, USDB, and W-*sd*-shell interactions. Figure (2) shows the *sd*-shell model space (MS) form factors for USDA interaction with g-free (black solid curve). The contributions of M1 (dashed curve) and M3 (dashed-dot curve) components are also indicated. The contributions of E0 and E2 were negligibly small. The inclusion of the center of mass correction (green curve) increased the total form factors at a high range of q value. The M1 component has a first diffraction minimum at q~0.9 fm^{-1} and at q~2.1 fm^{-1}, while the M3 component dominated along the momentum transfer range (0.5 < q < 1.7) fm^{-1} and has a diffraction minimum at q~1.9 fm^{-1}. The magnetic form factors for three *sd*-shell interactions

were similar, with a small difference in diffraction minimum, as shown in Figure (3). There was some dependence of the calculated form factors on the interaction. The interactions of USDB (grass green dashed curve) and W (orange curve) were identical, but USDA interaction (green curve) varied slightly in diffraction minimum. The core polarization effects were included through the effective g-factors with the typical values [15]: $g_l^p = 1.15$. $g_l^n = -0.15$. $g_s^p = 4.748$. $g_s^n = -3.252$. This inclusion is displayed in Figure (4) for different interactions; USDA (black curve), USDB (blue curve), and W (magenta curve). The measured magnetic moments $\mu_{exp.}$ = 1.53195(7) nm [30] were very well reproduced with g-free for all dependent interactions in magnitude with opposite sign, especially with USDB interaction, the values μ_{USDA} = -1.51395 nm, μ_{USDB} = -1.53167 nm and μ_W = -1.56795 nm, as tabulated in Table 1. The inclusion of the core polarization effect enhanced the calculated values to be μ_{USDA} = -1.60237 nm, μ_{USDB} = -1.61673 nm and μ_W = -1.64615 nm.

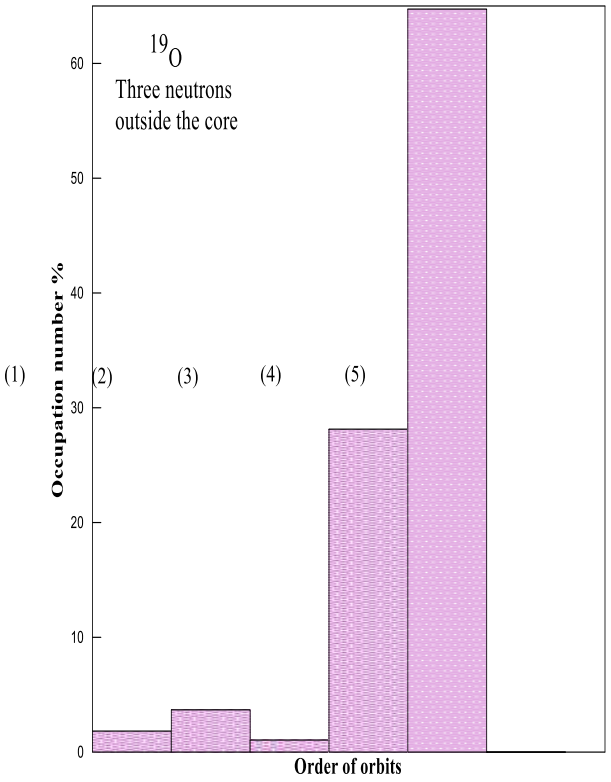

(1) $1d_{3/2}$=1, $1d_{5/2}$=2, $2s_{1/2}$=0 (4) $1d_{3/2}$=0, $1d_{5/2}$=2, $2s_{1/2}$=1
(2) $1d_{3/2}$=1, $1d_{5/2}$=1, $2s_{1/2}$=1 (5) $1d_{3/2}$=0, $1d_{5/2}$=3, $2s_{1/2}$=0

Figure 1: The occupation numbers percentage for the ground states of $1d_{5/2}$, $2s_{1/2}$, and $1d_{3/2}$ orbits outside the ^{16}O core of the considered ^{19}O nucleus.

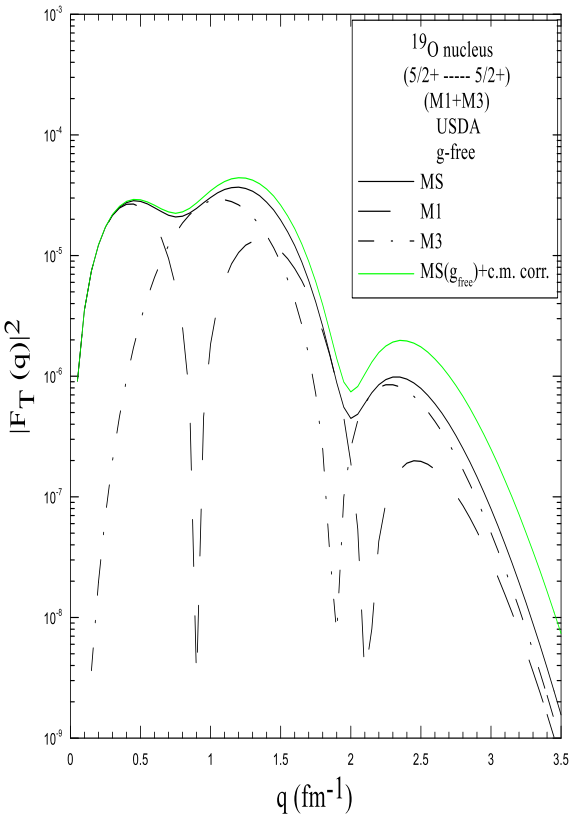

Figure 2: The transverse form factors for ^{19}O ground state calculated in *sd*-model space (black solid curve) and with $g_{(free)}$+c.m. corr. (green curve). The individual multipole contributions of M1 and M3 are shown.

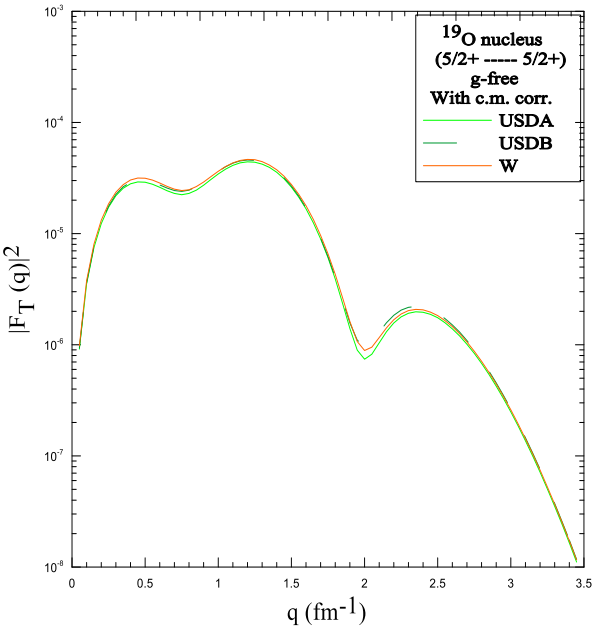

Figure 3: Comparison between the total form factors of ^{19}O nucleus with $g_{(free)}$+c.m. corr. for USDA (green curve), USDB (grass green dashed curve), and W-interaction (orange curve).

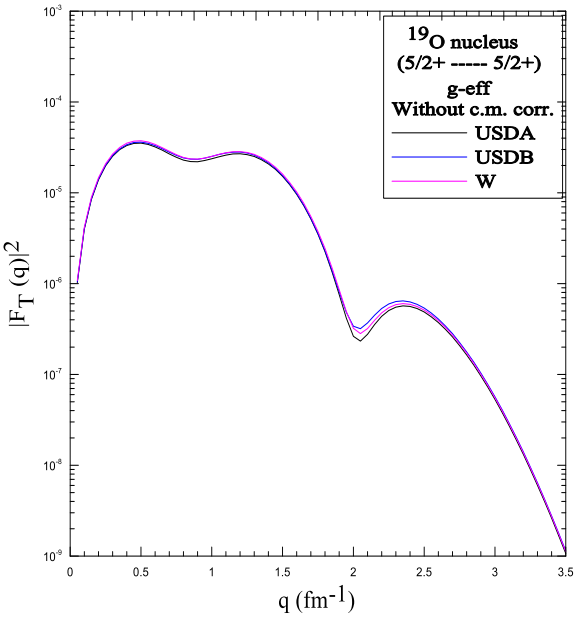

Figure 4: Comparison between the total form factors of ^{19}O nucleus with $g_{(eff.)}$ for the USDA (black curve), USDB (blue curve), and W-interaction (magenta curve).

3.2 ^{19}O nucleus ($J^{\pi}T = 3/2^{+}3/2$, $\tau_{1/2} = 1.37$ s)

The excited state ($E_x = 0.096$ MeV) of the ^{19}O nucleus (neutron-rich) is described by $J^{\pi}T$ $3/2^{+}3/2$, with a half-life of $\tau_{½} = 1.37$ s [30], so there is very little experimental data on this state. Figure (5) (solid curve) shows the calculated inelastic transverse form factors for *sd*-shell model space (MS) with b = 1.833 fm using universal *sd*-shell interaction A (USDA). The individual components M1 (dashed curve), M3 (dashed-dot curve), and the contribution of the center of mass correction (green curve) were indicated. It is interesting to note that the contributions of E2 and E4 were marginal in the total form factors. As shown in Figure (6) (green curve), the inclusion of the cm corr. increased the magnetic form factors at q > 1.7 fm^{-1}. The M3 component dominated the region around q~1.1 fm^{-1} with a diffraction minimum around q~2.0 fm^{-1}, while the M1 component was marginally moved backwards with the first diffraction maximum position around q~0.5 fm^{-1} and two diffraction minima at q~1.0 fm^{-1} and q~2.6 fm^{-1}, respectively. The inelastic magnetic form factors with g-free and with the exact cm corr. are displayed in Figure (6) for the different interactions: USDA (green curve), USDB (grass green dashed curve), and W (orange curve). The inclusion of the exact cm corr. led to a visible enhancement in the form factors at high q-region. The results of USDA and USDB were similar with minor differences for the W result. The contributions of the effective g-factors with the typical values of Richter et al. [15] are depicted in Figure (7) for USDA (black curve), USDB (blue curve), and W-interaction (magenta curve). These interactions gave essentially the same results for the form factors. The calculated magnetic moments with g-free for three *sd*-shell interactions ($\mu_{USDA} = 0.23$ nm, $\mu_{USDB} = 0.23714$ nm and $\mu_W = -0.18129$ nm,) underestimated the measured value $\mu_{exp.} = -0.72(9)$ nm [30] by a factor of about 3.1. The discrepancy increased with $g_{eff.}$to be $\mu_{USDA} = 0.18669$ nm, $\mu_{USDB} = 0.19224$ nm and $\mu_W = -0.14206$ nm. The sign was correctly reproduced only for W-interaction (see Table 1).

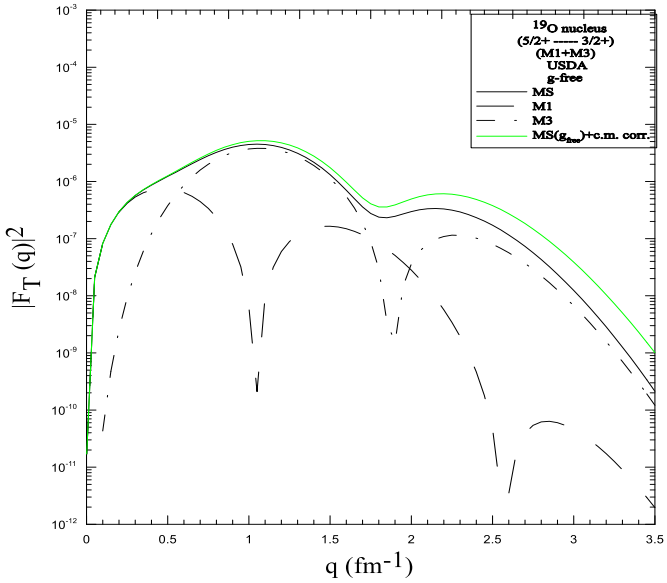

Figure 5: The transverse form factors for ^{19}O excited state calculated in *sd*-model space (black solid curve) and with $g_{(free)}$+c.m. corr. (green curve). The individual multipole contribution of M1 and M3 are shown.

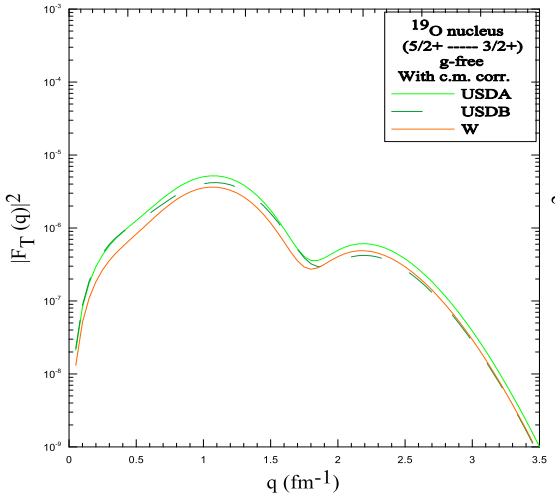

Figure 6: Comparison between the total form factors of ^{19}O nucleus with $g_{(free)}$+c.m. corr. for USDA (green curve), USDB (grass green dashed curve), and W-interaction (orange curve).

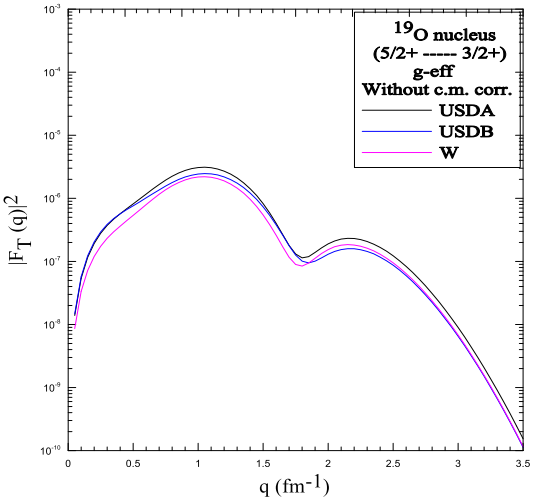

Figure 7: Comparison between the total form factors of ^{19}O nucleus with $g_{(eff.)}$ for the USDA (black curve), USDB (blue curve), and W-interaction (magenta curve).

3.3 ^{21}Na nucleus ($J^{\pi}T$ = 3/2^{+}1/2, $\tau_{1/2}$ = 22.5 s)

The ground state of the exotic ^{21}Na nucleus was characterized by $J^{\pi}T$, 3/2^{+}1/2, with a half-life of $\tau_{½}$ = 22.5 s [30]; experimental data are scarce for this state. The ground state of the ^{21}Na nucleus can be regarded as a core of ^{16}O with five nucleons distributed over $1d_{5/2}$, $2s_{1/2}$, and

$1d_{3/2}$ orbits. The configurations used to describe the ground state of the ^{21}Na nucleus are $(1s)^4$, $(1p_{3/2})^8$, $(1p_{1/2})^4$ inert core, with USDA interaction [15] are shown in Figure (8). The calculated magnetic form factors of the *sd*-shell model space (MS) with b = 1.845 fm are presented in Figure (9) (black solid curve) for USDA interaction. The individual components M1 (dashed curve) and M3 (dashed-dot curve) are shown. It is worth noting that E0 and E2 components have negligibly small total form factor contributions. The M3 component dominated the q~1.2 fm^{-1} region, while the M1 component moved backwards with the diffraction maximum location around q~0.5 fm^{-1}. In the region of (0.5 < q < 2.0) fm^{-1}, the total magnetic form factor was almost totally M3 transition. For the M1 component, two diffraction minima appeared at q~1.1 fm^{-1} and q~2.5 fm^{-1}, respectively; while the M3 component has just one diffraction minimum at q~2.15 fm^{-1}. The contribution of the exact center of mass correction increased the transverse magnetic form factors at (q > 1.9) fm^{-1} region, as illustrated in Figure (9) (green curve). There was some dependence of the calculated magnetic form factors with the exact center of mass correction and g-free on the interactions USDA, USDB, and W along the region of momentum transfer (2.3 < q < 3.0) fm^{-1}, as shown in Figure (10). The typical values of the effective g-factors [15] showed a small dependence of the magnetic form factors on the interaction. Comparison is shown in Figure (11) for the interactions; USDA (black curve), USDB (blue curve), and W (magenta curve). While $g_{eff.}$ has a good role in the magnetic moment values. The calculated magnetic moments with g-free μ_{USDA} = 2.47923 nm, μ_{USDB} = 2.48911 nm and μ_W = 2.55426 nm were close to the measured value $\mu_{exp.}$ = 2.38630(10) nm [30] with some enhancement. With effective g-factors, the calculated value was very well reproduced for all interactions as tabulated in Table 1, μ_{USDA} = 2.35474 nm, μ_{USDB} = 2.36209 nm and μ_W = 2.42534 nm.

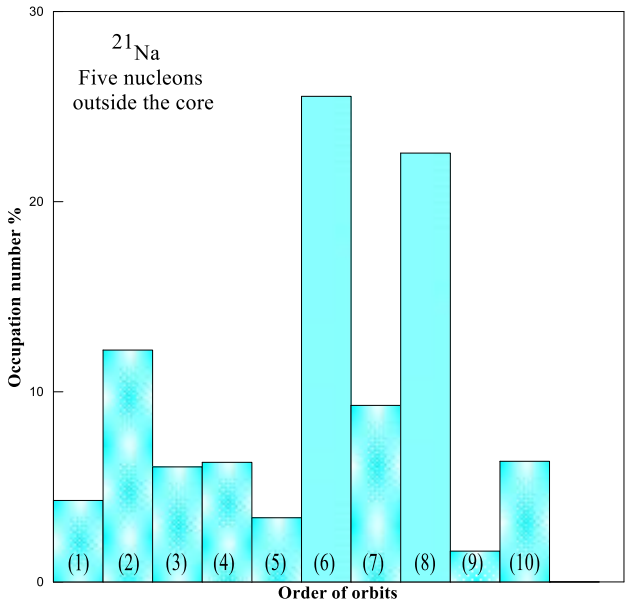

(1) $1d_{3/2}$=2, $1d_{5/2}$=2, $2s_{1/2}$=1 (6) $1d_{3/2}$=0, $1d_{5/2}$=4, $2s_{1/2}$=1
(2) $1d_{3/2}$=1, $1d_{5/2}$=3, $2s_{1/2}$=1 (7) $1d_{3/2}$=0, $1d_{5/2}$=3, $2s_{1/2}$=2
(3) $1d_{3/2}$=2, $1d_{5/2}$=3, $2s_{1/2}$=0 (8) $1d_{3/2}$=0, $1d_{5/2}$=5, $2s_{1/2}$=0
(4) $1d_{3/2}$=1, $1d_{5/2}$=4, $2s_{1/2}$=0 (9) $1d_{3/2}$=1, $1d_{5/2}$=1, $2s_{1/2}$=3

Figure 8: The occupation numbers percentage for the ground states of 1d5/2, 2s1/2, and 1d3/2 orbits outside the 16O core of the considered 12Na nucleus.

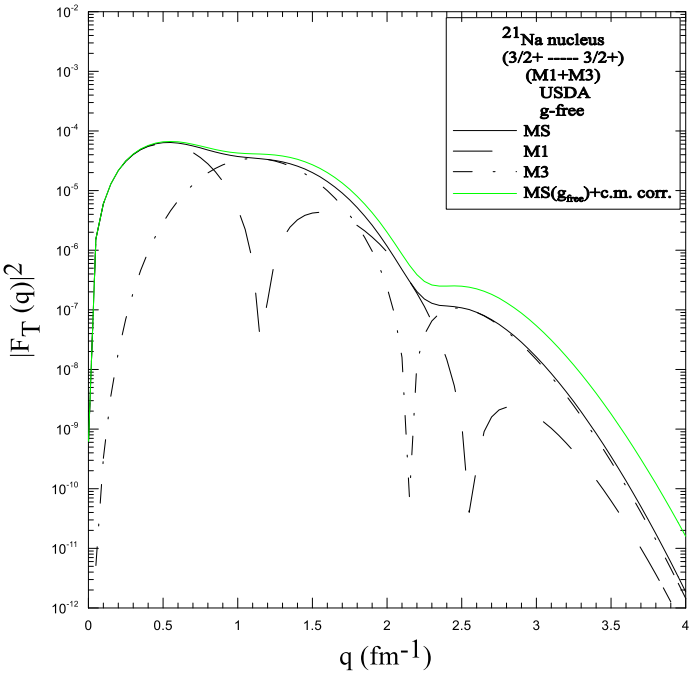

Figure 9: The transverse form factors for ^{21}Na ground state calculated in *sd*-model space (black solid curve) and with $g_{(free)}$+c.m. corr. (green curve). The individual multipole contribution of M1 and M3

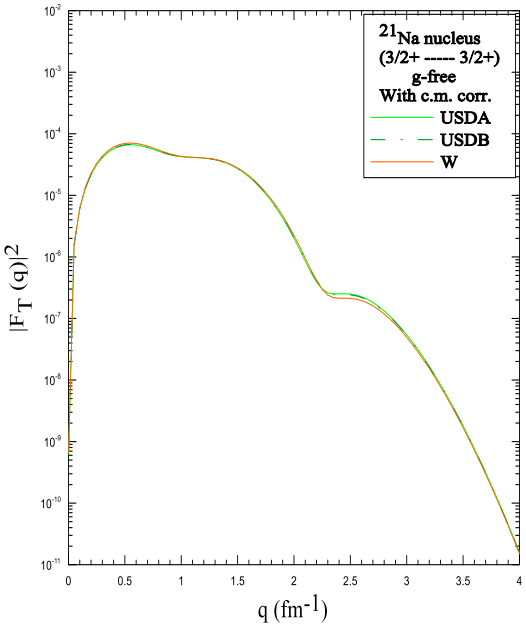

Figure 10: Comparison between the total form factors of ^{21}Na nucleus with $g_{(free)}$+c.m. corr. for USDA (green curve), USDB (grass green dashed curve), and W-interaction (orange curve).

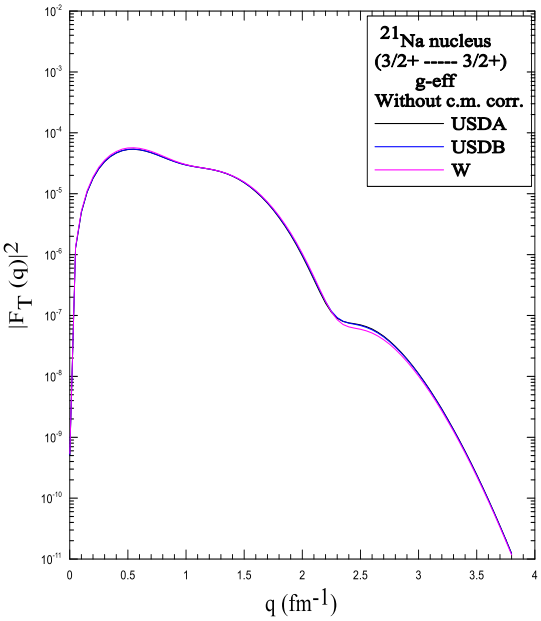

Figure 11: Comparison between the total form factors of ^{21}Na nucleus with $g_{(eff.)}$ for the USDA (black curve), USDB (blue curve), and W-interaction (magenta curve).

3.4 ^{21}Na nucleus ($J^{\pi}T = 5/2^{+}1/2$, $\tau_{1/2} = 6.9$ ps)

The excited state of the ^{21}Na exotic nucleus ($E_x = 0.332$ MeV) was characterized by $J^{\pi}T = 5/2^{+}1/2$ with a half-life of $\tau_{½} = 6.9$ ps [30], so there is no experimental data for this state. The calculated transverse form factors for *sd*-shell model space (MS) with g_{free} and USDA interaction are shown in Figure (12) (black solid curve). The individual components M1 (dashed curve), M3 (dashed-dot curve), and the effect of the exact center of mass correction (green curve) are displayed. There was no contribution for E2 and E4 components. The M1 component has two diffraction minima located at q~1.0 fm^{-1} and q~2.1 fm^{-1}, respectively, while the M3 component has only one diffraction minimum at q~3 fm^{-1}. The magnetic form factor was totally M1 at q < 0.7 fm^{-1}. In the region of q along (0.8 < q < 2.2) fm^{-1}, the magnetic total form factor is attributed to M3 contribution with some percentage of M1 contribution. The inclusion of the exact cm corr. (green curve) enhanced the total magnetic form factors along the range of momentum transfer for q > 1.5 fm^{-1}. The dependence of the magnetic form factors with the exact cm corr. (green curve) on these different interactions are shown in Figure (13). The result of USDA interaction (green curve) distinctly differed from that of USDB (grass green dashed curve) and W (orange curve), which were identical. The core polarization effects are shown in Figure (14) for the different interactions: USDA, USDB, and W. The effective g-factor had a minor dependence on the form factors and played a significant role in the magnetic moment values compared with that of the g-free. The calculated magnetic moments with g-free for μ_{USDA} = -0.8944 nm, μ_{USDB} = -0.79442 nm and μ_{W} = -0.79444 nm underestimated the measured value $\mu_{exp.}$ = 3.7(3) nm [30] by a factor of 4.1 with an opposite sign. The discrepancy increased with

$g_{eff.}$to be μ_{USDA} = -0.70802 nm, μ_{USDB} = -0.70624 nm and μ_W = -0.70167 nm. The comparison of the calculated and measured magnetic moments with other results is tabulated in Table 1.

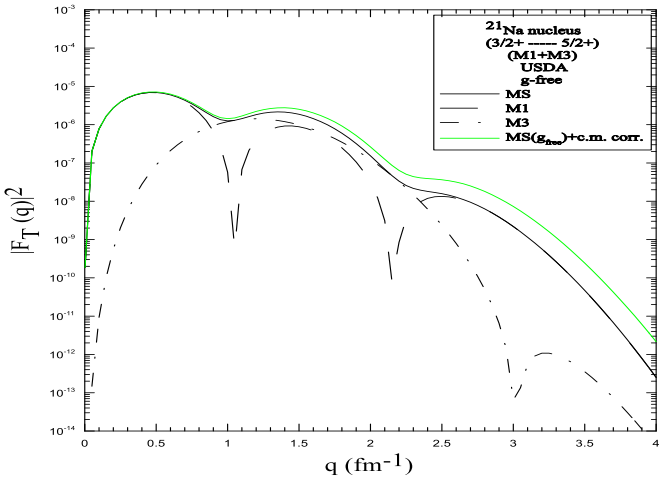

Figure 12: The transverse form factors for ^{21}Na excited state calculated in *sd*-model space (black solid curve) and with $g_{(free)}$+c.m. corr. (green curve). The individual multipole contribution of M1 and M3 are shown.

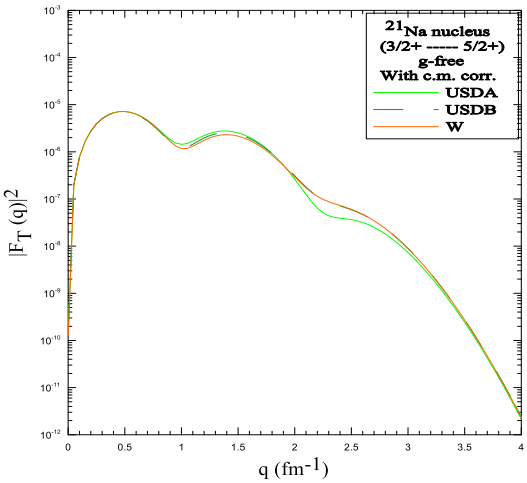

Figure 13: Comparison between the total form factors of ^{21}Na nucleus with $g_{(free)}$+ c.m. corr. for USDA (green curve), USDB (grass green dashed curve), and W-interaction (orange curve).

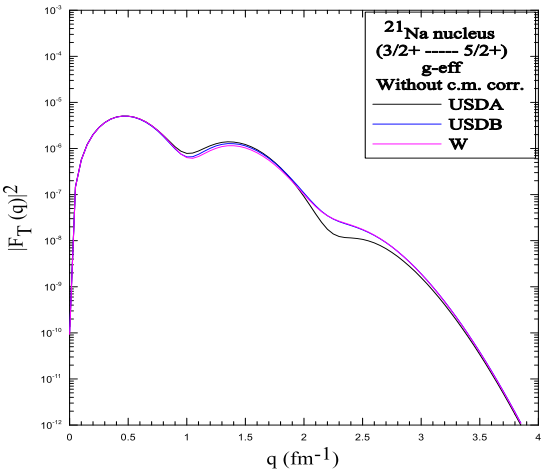

Figure 14: Comparison between the total form factors of ^{21}Na nucleus with $g_{(eff.)}$ for the USDA (black curve), USDB (blue curve), and W-interaction (magenta curve).

Table 1: The calculated magnetic dipole moments (μ) of ^{19}O and ^{21}Na nuclei are compared with experimental data of Ref. [30] and with other results.

Nucleus	J^{π}	***E_x (KeV)***	***Technique***	***$\mu_{calc.}$ (nm)***			***$\mu_{exp.}$ (nm)***	***Other results***
				USDA interaction	***USDB interaction***	***W interaction***		
^{19}O	$5/2^{+}$	0	g(free)	-1.51395	-1.53167	-1.56795	1.53195(7)	-1.531[31]
			g(eff.)[(a)]	-1.60237	-1.61673	-1.64615		
^{19}O	$3/2^{+}$	96	g(free)	0.23	0.23714	-0.18129	-0.72(9)	-0.945[31]
			g(eff.)	0.18669	0.19224	-0.14206		
^{21}Na	$3/2^{+}$	0	g(free)	2.47923	2.48911	2.55426	2.38630(10)	2.489[31] 2.137[32]
			g(eff.)	2.35474	2.36209	2.42534		
^{21}Na	$5/2^{+}$	332	g(free)	-0.8944	-0.79442	-0.79444	3.7(3)	3.355[31]
			g(eff.)	-0.70802	-0.70624	-0.70167		

[(a)]g(eff): $g_l^p = 1.15.\ g_l^n = -0.15.\ g_s^p = 4.748.\ g_s^n = -3.252$

4. Conclusions

The main conclusions for the current work can be drawn from the following:

1. The magnetic dipole moment did not depend on the size parameter b.
2. The exact center of mass correction did not affect the magnetic dipole moments, but some enhancement was noticed for q-depend form factors.
3. Since ^{19}O and ^{21}Na are exotic nuclei near the stability line, all three *sd*-shell interactions gave a similar description of the magnetic transition form factors.
4. The measured magnetic dipole moment of the ground state of ^{19}O was well reproduced with USDB interaction by free g-factors, while that of ^{21}Na was well reproduced by the effective g-factors.
5. The magnetic dipole moment of the excited state of ^{19}O underestimated the experimental data but with the same sign.
6. Predictions of the magnetic dipole moments provide a discriminating test and can lead to improving the wave functions.

References

[1] J. D. Walecka, "Overview of the CEBAF Scientific program," *A.I.P. Con. Proc. 269,* pp. 87 1992, eds. F. Gross and R. Holt, A.I.P., New York, pp. 97, 1993.

[2] R. A. Radhi, Z. A. Dakhil and B. S. Hameed, "Elastic and Inelastic Magnetic Electron Scattering Form Factors of Neutron-Rich ^{13}C Exotic Nucleus," *Iraqi Journal of Science,* vol. 55, no. 4B, pp. 1859-1867, 2014.

[3] I. Tanihata H. Hamagaki, O. Hashimoto, Y. Shida, N. Yoshikawa, K. Sugimoto, O. Yamakawa, T. Kobayashi, N. Takahashi, "Measurements of Interaction Cross Sections and Nuclear Radii in the Light *p*-Shell Region," *Phys. Rev. Lett.*, vol. 55, no. 24, pp. 2676, 1985.

[4] K. Hagino, I. Tanihata, and H. Sagawa, in "100 Years of Subatomic Physics," edited by E. M. Henley and S. D. Ellis, (World Scientific, Singapore), pp. 231-272, 2013.

[5] M. H. Hawi and Z. A. Dakhil, "Electromagnetic Form Factors for ^{7,9,11}Be Isotopes with Exact Center of Mass Correction," *Iraqi Journal of Science,* vol. 63, no. 1, pp. 149-162, 2022.

[6] P. Descouvemont, "Low-energy ^{11}Li+*p* and ^{11}Li+*d* scattering in a multicluster model," *Phys. Rev. C,* vol. 101, 064611, 2020.

[7] Shan-Gui Zhou, "Structure of Exotic Nuclei: A Theoretical Review," *The 26th Intl. Nucl. Phys. Con.*, Adelaide, Australia, 11-16 September, 2016, Proceedings of Science, 2017.

[8] D. H. Jakubassa-Amundsen, "Elastic scattering of spin-polarized electrons and positrons from ^{23}Na nuclei," *Nucl. Phys. A,* vol. 975, pp. 107-121, 2018.

[9] P. Sarriguren, D. Merino, O. Moreno, E. Moya de Guerra, D. N. Kadrev. A. N. Antonov and M. K. Gaidrov, "Elastic magnetic electron scattering from deformed nuclei," *Phys. Rev. C,* vol. 99, 034325, 2019.

[10] P. Sarriguren, O. Moreno, E. Moya de Guerra, D. N. Kadrev, A. N. Antonov, and M. K. Gaidarov, "Elastic Magnetic Electron Scattering from Odd-A Nuclei," *J. of Physics: Con. Series,* 1555, 012001, 2020.

[11] S. Hudan, R. T. deSouza, A. S. Umar, Z. Lin, and C. J. Horowitz, "Enhanced dynamics in fusion of neutron rich-oxygen nuclei at above-barrier energies," *Phys. Rev. C,* vol 101, 061601 (R), 2020.

[12] B. H. Wildenthal, "Empirical Strengths of Spin Operators in Nuclei," *Prog. in Part. and Nucl. Phys.*, vol. 11, pp. 5-51, 1984.

[13] B. A. Brown and B. H. Wildenthal, "Status of the Nuclear Shell Model," *Ann. Rev. Nucl. Part. Sci.*, vol. 38, pp. 29-66, 1988.

[14] B. Alex Brown and W. A. Richter, "New "USD" Hamiltonians for the *sd* shell," *Phys. Rev. C,* vol. 74, 034315, 2006.

[15] W. A. Richter, S. Mkhize, and B. Alex Brown, "*sd*-shell observables for the USDA and USDB Hamiltonians," *Phys. Rev. C,* vol. 78, 064302, 2008.

[16] Bogdan Mihaila and Jochen H. Heisenberg, "Center-of-mass corrections reexamined: A many-body expansion approach," *Phys. Rev. C,* vol. 60, 054303, 1999. Item., "Ground state correlations and mean field in ^{16}O. II. Effects of a three-nucleon interaction," *Phys. Rev. C,* vol. 61, 054309, 2000. Item., "Microscopic Calculation of the Inclusive Electron Scattering Structure Function in ^{16}O," *Phys. Rev. Lett.*, vol. 84, no. 7, pp. 1403, 2000.

[17] T. William Donnelly and Ingo Sick, "Elastic magnetic electron scattering from nuclei," *Rev. of Mod. Phys.*, vol. 56, no. 3, pp. 461-566, 1984.

[18] J. P. Elliot and T. H. R. Skyrme, "Centre-of-Mass Effects in the Nuclear Shell-Model," *Proc. R. Soc. Lond. A,* 232, pp. 561-566, 1955.

[19] L. J. Tassie and F. C. Barker, "Application to Electron Scattering of Center-of-Mass Effects in the Nuclear Shell Model," *Phys. Rev.*, vol. 111, no. 3, pp. 940, 1958.

[20] J. P. Glickman, W. Bertozzi, T. N. Buti, S. Dixit, F. W. Hersman, C. E. Hyde-Wright, M. V. Hynes, R. W. Lourie, B. E. Norum, J. J. Kelly, B. L. Berman, and D. J. Millener, "Electron Scattering from ^{9}Be," *Phys. Rev. C,* vol. 43, no. 4, pp. 1740, 1991.

[21] P. J. Brussaard and P. W. M. Glademans, "Shell-model Application in Nuclear Spectroscopy", North-Holland Publishing Company, Amsterdam, 1977.

[22] B. A. Brown, R. A. Radhi and B. H. Wildenthal, "Electric Quadrupole and Hexadecupole Nuclear Excitations from the Perspectives of Electron Scattering and Modern Shell-Model Theory," *Phys. Rep. (Rev. Sec. of Phys. Lett.),* vol. 101, no. 5, pp. 313-358, 1983.

[23] I. S. Towner, "A Shell Model Description of Light Nuclei", Oxford Studies in Nuclear Physics, Clarendon Press, Oxford, 1971.

[24] B. A. Brown, B. H. Wildenthal, C. F. Williamson, F. N. Rad, S. Kowalski, Hall Crannell, and J. T. O'Brien, "Shell-model analysis of high-resolution data for elastic and inelastic electron scattering on ^{19}F," *Phys. Rev. C,* vol. 32, no. 4, pp. 1127-1156, 1985.

[25] B. A. Brown, W. Chung and B. H. Wildenthal, "Inelastic scattering *E* 4 transition probabilities in the 0*d*, 1*s* shell," *Phys. Rev. C,* vol. 21, no. 6, pp. 2600, 1980.

[26] H. Überall, "Electron Scattering from Complex Nuclei", *Academic Press,* New York, 1971.

[27] A. G. Sitenko and V. K. Taratakovskii, "Lectures on the Theory of the Nucleus", *Pergamon Press,* Oxford, 1975.

[28] Herman Feshbach, Avraham Gal and Jörg Hüfner, "On high-energy scattering by nuclei__II," *Ann. Phys.*, vol. 66, pp. 20-59, 1971.

[29] B. A. Brown, A. Etchgoyen, N. S. Godwin, W. D. M. Rae, W. A. Richter, W. E. Ormand, E. K. Warburton, J. S. Winfield, L. Zhao, and C. H. Zimmerman, *MSU-NSCL report number 1289*, 2005.

[30] N. J. Stone, "Table of nuclear magnetic dipole and electric quadrupole moments", International Nuclear Data Committee, International Atomic Energy Agency (IAEA), INDC (NDS), 0658, Vienna, Austria, 2014.

[31] Archana Saxena and Praveen C. Srivastava, "First-principles results for electromagnetic properties of *sd* shell nuclei," *Phys. Rev. C*, vol. 96, 024316, 2017.

[32] J. G. Pronko, R. A. Lindgren and D. A. Bromley, "Structure of ^{21}Na from the ^{24}Mg(p,α)^{21}Na Reaction," *Nucl. Phys. A*, vol. 140**,** pp. 465-480, 1970.